Optimal Control Strategy of a Series-Connected Multimachine System Supplied by a Single Inverter Using Third-Order Sliding-Mode Algorithm

Faycal Mehedi[1,*], Abdelkader Yousfi[2], Ismail Bouyakoub[1], Zakaria Reguieg[1]
[1]Laboratoire Genie Electrique et Energies Renouvelables (LGEER), Faculty of Technology, Hassiba Benbouali University of Chlef, Chlef 02000, Algeria
[2]Laboratory LAGC, Faculty of Science and Technology, Djilali Bounaama University of Khemis Miliana, Khemis Miliana, Algeria
[*]f.mehedi@univ-chlef.dz; a.yousfi@univ-dbkm.dz; i.bouyakoub@univ-chlef.dz; z.reguieg@univ-chlef.dz

***Abstract*—This paper presents a robust control strategy for multimachine systems (MMSs) composed of two five-phase permanent magnet synchronous motors (5Ph-PMSMs) connected in series through their stator windings. A single five-phase inverter can drive both machines while ensuring independent regulation using a phase transposition scheme. Conventional vector control with proportional-integral (PI) regulators is sensitive to parameter variations, whereas classical sliding mode control (SMC) suffers from chattering, transient errors, and reduced robustness. To address these issues, an advanced method based on third-order sliding mode control (TOSMC) is proposed for speed and current regulation. The approach was tested in MATLAB/Simulink, showing clear improvements. For 5Ph-PMSM1, the response time decreased by 45.29 % compared to MMS-SMC and 84.16 % compared to the PI-based control; for 5Ph-PMSM2, the reductions were 32.25 % and 81.73 %, respectively. Torque ripple was also reduced, reaching 9 % and 75.40 % for 5Ph-PMSM1, and 9.3 % and 76.03 % for 5Ph-PMSM2, relative to the MMS-PI and MMS-SMC technique. These results demonstrate the robustness and high efficiency of the proposed MMS-TOSMC method, which makes it suitable for demanding MMS drive applications.**

***Index Terms*—Five-phase PMSM; Multimachine systems; Robustness; Series-connected; Third-order sliding mode control.**

I. INTRODUCTION

Multiphase machines (MPMs) are gaining greater use in various fields [1]–[3]. To meet these growing demands, such systems must deliver reliable operation and sustained efficiency, even under varying load conditions and external disturbances. Compared to conventional three-phase configurations, MPMs provide notable advantages, including enhanced reliability and efficiency, reduced current in each phase, diminished torque ripple, greater power handling capability, and more stable speed regulation [4]–[6]. A key benefit is the tolerance of the system fault, which allows it to continue running with only a slight performance loss and low torque ripple. This dependability is crucial in industry, where a propulsion failure can compromise safety, be very expensive, and disrupt operations [7].

A principal advantage of modern multiphase systems is their support for multimotor arrangements powered by a single converter. Emerging studies, building on progress in this technology, are exploring such series and parallel setups primarily to minimise weight without sacrificing output. In these configurations, each motor remains independently controllable despite the shared power source [8], [9].

In multiphase drive control, torque and flux are managed solely by the d and q current components. This strategy deliberately frees the other components, enabling the control of multiple machines from one shared inverter. However, independent control of series-connected machines depends on a custom-designed coupling [10]. To achieve independent control of machines in a series configuration, a specific coupling method involving a deliberate phase transposition is essential. Research has shown that when this correct phase transposition is implemented, the resulting current components enable the independent operation of each machine [11]. According to [10], this configuration significantly boosts operational robustness. The investigation demonstrated that sophisticated control algorithms could keep dual machines running at consistent speed, even following an inverter open-phase fault, thereby ensuring system continuity.

The MPMs are primarily accomplished through established techniques such as vector control (VC) and direct torque control (DTC) [12]–[15]. A key limitation of VC, which commonly employs proportional-integral (PI) regulators, is its performance trade-off: despite offering rapid dynamics, it results in undesirable high current total harmonic distortion (THD), noticeable torque ripple, and compromised robustness in MPM systems [16], [17]. This has motivated significant research into nonlinear control schemes to supersede conventional PI-based methods, with promising results from approaches such as fuzzy logic control [18], predictive control [19], and genetic algorithms [20].

Manuscript received 14 May, 2025; accepted 30 July, 2025.

Sliding mode control (SMC) is valued for its stability and rapid response when facing system uncertainties and disturbances. However, its main drawback is the chattering effect [21]–[23]. To mitigate these inherent limitations, researchers have proposed several advanced control schemes. These refinements, which seek to augment the efficacy of traditional SMC, encompass the implementation of fuzzy logic within SMC [24], a synergetic controller fused with SMC [25], and the incorporation of backstepping technique principles [26].

Higher-order SMC (HOSMC) offers a solution to the persistent chattering problem of conventional SMC. Its key innovation is to direct the discontinuous control action toward the higher-order derivatives of the sliding variable, rather than the variable itself, which significantly reduces chattering. A widely adopted variant is second-order SMC (SOSMC), which has been proven to be an effective and practical substitute for standard SMC [27]. Illustratively, research in [28] employed a SOSMC strategy to improve the regulation of a five-phase induction motor. This approach provided robustness against system uncertainties without introducing excessive complexity.

To address the drawbacks typically associated with conventional sliding mode control, the third-order SMC (TOSMC) method was introduced [13]. This advanced scheme has shown a strong capability in handling systems affected by disturbances and modelling inaccuracies, offering a reliable solution that strengthens performance in both linear and nonlinear environments.

The original contribution of this research lies in addressing the control of series-connected multimachine systems driven by a single inverter, with emphasis on achieving effective decoupling, faster dynamic response, reduced torque ripple, and improved resilience to parameter variations. The main contributions can be summarised as follows:

– Implementation of a robust decoupling strategy for series-connected five-phase permanent magnet synchronous motors (5Ph-PMSMs) supplied by a f single inverter;

– The proposed multimachine system (MMS)-TOSMC method demonstrates higher efficiency and reliability in multimachine control compared with existing approaches;

– The strategy successfully minimises torque ripple in both motors, outperforming alternatives such as MMS-SMC in reducing chattering effects;

– Enhanced multimachine system control performance is achieved, including reduced rotor speed tracking errors, shorter response times, and stronger robustness against machine parameter uncertainties.

This article is organised in a systematic manner to present the main aspects of the study. Section II describes the process of configuring and modelling series-connection of two five-phase PMSMs along with their vector control technique. Section III explains the application of SMC to series-connected motors. Section IV introduces the proposed TOSMC-based MMS control scheme, designed for two series-linked 5Ph-PMSMs driven by a single inverter. Section V presents the simulation results of the proposed technique and contrasts them with conventional methods. Finally, Section VI provides the conclusions of the work.

II. MODELLING AND DECOUPLED CONTROL OF A MULTIMACHINE SYSTEM

The system under investigation comprises two 5Ph-PMSMs. As depicted in Fig. 1, the five-phase stator windings of both machines are connected in series, incorporating a phase transposition [9]. This transposition is a deliberate design element to ensure that the magneto-motive force (mmf) produced by the second machine is the spatial inverse of the force produced by the first machine, and vice versa. The described system architecture allows for independent control of each machine. A five-leg inverter provides electrical power to the system via its five output phases (v_a, v_b, v_c, v_d, v_e) [10]. These outputs connect to the machine phases, identified as v_{as}, v_{bs}, v_{cs}, v_{ds}, and v_{es}, which reflect the spatial distribution of their windings depicted in Fig. 1.

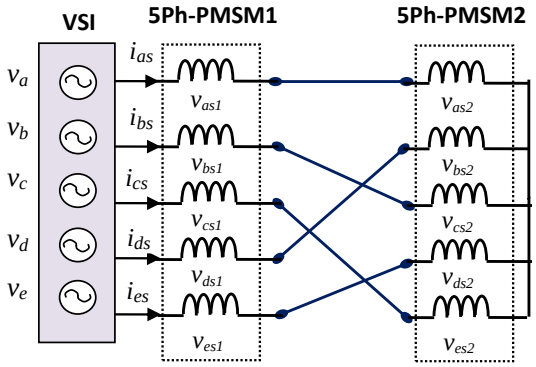

Fig. 1. Topology of two series-connected 5Ph-PMSMs fed by a single five-phase inverter.

The configuration shown in Fig. 1 demonstrates that the output voltage of the inverter, measured with respect to the neutral point, corresponds to the combined winding voltages of both machines. This relationship can be formulated using vector representation [11]

$$[V^s] = \begin{bmatrix} v_a \\ v_b \\ v_c \\ v_d \\ v_e \end{bmatrix} = \begin{bmatrix} v_{as1} + v_{as2} \\ v_{bs1} + v_{cs2} \\ v_{cs1} + v_{bs2} \\ v_{ds1} + v_{bs2} \\ v_{es1} + v_{ds2} \end{bmatrix}. \quad (1)$$

The currents obtained at the inverter output terminals can be described by the following mathematical expressions

$$[I^s] = \begin{bmatrix} i_a \\ i_b \\ i_c \\ i_d \\ i_e \end{bmatrix} = \begin{bmatrix} i_{as1} \\ i_{bs1} \\ i_{cs1} \\ i_{ds1} \\ i_{es1} \end{bmatrix} = \begin{bmatrix} i_{as2} \\ i_{cs2} \\ i_{es2} \\ i_{bs2} \\ i_{ds2} \end{bmatrix}. \quad (2)$$

A fundamental tenet of independent vector control is that, through an appropriate stator winding arrangement in a multiphase machine, two distinct current components can be used to independently regulate the magnetic flux and the electromagnetic torque.

The voltage-current relationships for both motors are defined by the following equations, which are formulated in

the rotational d-q reference frame [11]:

$$\begin{cases} v_{ds1} = (R_{s1} + R_{s2})i_{ds1} + \left(L_{d1} + L_{sl2}\right)\dfrac{d}{dt}i_{ds1} - w_{r1}L_{q1}i_{qs1}, \\ v_{qs1} = (R_{s1} + R_{s2})i_{qs1} + \left(L_{q1} + L_{sl2}\right)\dfrac{d}{dt}i_{qs1} + w_{r1}L_{d1}i_{ds1} + \sqrt{\dfrac{5}{2}}w_{r1}\varphi_{f1}, \\ v_{ds2} = (R_{s1} + R_{s2})i_{ds2} + \left(L_{d2} + L_{sl1}\right)\dfrac{d}{dt}i_{ds2} - w_{r2}L_{q2}i_{qs2}, \\ v_{qs2} = (R_{s1} + R_{s2})i_{qs2} + \left(L_{q2} + L_{sl1}\right)\dfrac{d}{dt}i_{qs2} + w_{r2}L_{d2}i_{ds2} + \sqrt{\dfrac{5}{2}}w_{r2}\varphi_{f2}. \end{cases} \quad (3)$$

Here, $L_{d1} = L_{q1} = L_{sl1} + 5/2m_{s1}$, $L_{d2} = L_{q2} = L_{sl2} + 5/2m_{s2}$.

When two machines are linked in series, the overall torque is determined based on the separate current contributions delivered by the inverter:

$$\begin{cases} T_{e1} = p_1((L_d - L_q)i_d^{\,inv}i_q^{\,inv} + \sqrt{\dfrac{5}{2}}\varphi_{f1}i_q^{\,inv}), \\ T_{e2} = p_2((L_x - L_y)i_x^{\,inv}i_y^{\,inv} + \sqrt{\dfrac{5}{2}}\varphi_{f2}i_y^{\,inv}). \end{cases} \quad (4)$$

The mechanical dynamics equation of the two motors can be expressed as follows:

$$\begin{cases} J_{m1}\dfrac{dw_{r1}}{dt} = p_1T_{e1} - p_1T_{r1} - f_{m1}w_1, \\ J_{m2}\dfrac{dw_{r2}}{dt} = p_2T_{e2} - p_2T_{r2} - f_{m2}w_2. \end{cases} \quad (5)$$

In vector control applications, a common practice is to set the direct-axis current components (i_{ds1} and i_{ds2}) to zero. Doing so streamlines the control process, since only the quadrature-axis currents (i_{qs1} and i_{qs2}) are then used to regulate the system, as illustrated in Fig. 2 [11].

The voltage references are determined on the basis of the connection diagram presented in Fig. 1, where

$$\begin{bmatrix} v_a^* \\ v_b^* \\ v_c^* \\ v_d^* \\ v_e^* \end{bmatrix} = \begin{bmatrix} v_{as1}^* + v_{as2}^* \\ v_{bs1}^* + v_{cs2}^* \\ v_{cs1}^* + v_{es2}^* \\ v_{ds1}^* + v_{bs2}^* \\ v_{es1}^* + v_{ds2}^* \end{bmatrix}. \quad (6)$$

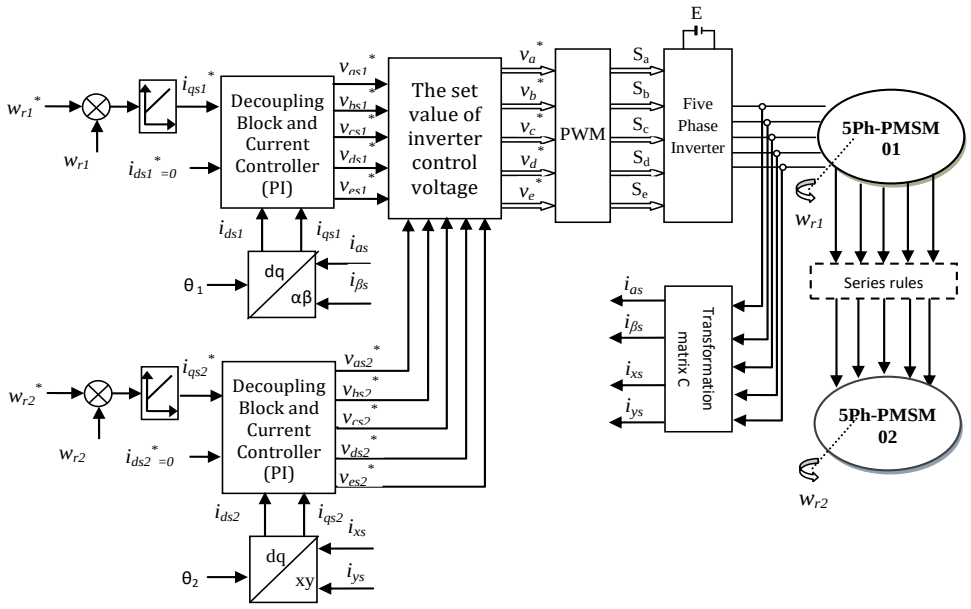

Fig. 2. Block diagram of vector control of two series-connected 5Ph-PMSMs.

Inverter phase current references are as follows:

$$\begin{bmatrix} i_a \\ i_b \\ i_c \\ i_d \\ i_e \end{bmatrix} = \begin{bmatrix} i_{as1} \\ i_{bs1} \\ i_{cs1} \\ i_{ds1} \\ i_{es1} \end{bmatrix} = \begin{bmatrix} i_{as2} \\ i_{cs2} \\ i_{es2} \\ i_{bs2} \\ i_{ds2} \end{bmatrix} = \begin{bmatrix} i_{as1}^* + i_{as2}^* \\ i_{bs1}^* + i_{cs2}^* \\ i_{cs1}^* + i_{es2}^* \\ i_{ds1}^* + i_{bs2}^* \\ i_{es1}^* + i_{ds2}^* \end{bmatrix}. \quad (7)$$

Equations (3) and (4) are fully decoupled, enabling independent control of each machine. One implemented method is a vector control strategy utilising PI controllers. This approach maintains the i_{ds1} and i_{ds2} current components at zero, allowing machine torques to be regulated exclusively via the i_{qs1} and i_{qs2} currents. As illustrated in the vector control diagram in Fig. 2, current controllers subsequently generate the complete voltage reference signals [11].

III. THE SMC STRATEGY FOR TWO SERIES-CONNECTED 5PH-PMSMS

Sliding mode control is regarded as a resilient strategy since it can sustain reliable performance even under system uncertainties, external disturbances, and dynamic variations. This robustness arises mainly from the distinctive features that define the method [22].

The initial phase of developing an SMC scheme involves specifying a set of switching functions *S(x)*. In this study, the sliding surface is represented by the following formulation [23], [24]:

$$S(x) = \left(\frac{d}{dt} + \lambda\right)^{n-1} e(x), \quad (8)$$

where n denotes the relative degree, λ is a positive coefficient, and e symbolises the tracking error vector $e = x^* - x$.

The next stage involves formulating the control law so that condition $\dot{S}(x) = 0$ is fulfilled, guaranteeing the convergence of the system to the sliding surface. The attractiveness requirement can then be expressed as [22]

$$S(x)\dot{S}(x) < 0. \tag{9}$$

The basic control law consists of two main sections

$$U = U_{eq} + U_n. \tag{10}$$

The control vector U is defined by its equivalent component (U_{eq}) and a correction factor (U_n). The calculation of U_n is essential to satisfy the stability criteria of the chosen control.

The control vector U comprises two elements: an equivalent component (U_{eq}) and a corrective component (U_n). Determining U_n is critical for the stability of the system [23]

$$U_n = K\ sat\ \left(\left(S(x)/\delta\right)\right), \tag{11}$$

where K is a constant.

The $sat\ \left(\left(S(x)/\delta\right)\right)$ represents the saturation function, and the parameter δ specifies the thickness of the boundary layer.

In this work, the sliding surface is formulated based on the deviation between the reference and measured speeds, together with the corresponding current components of the two 5Ph-PMSMs. Accordingly, the mathematical expression is given below.

For the first machine:

$$\begin{cases} S(i_{ds1}) = i_{ds1}^{\ *} - i_{ds1}, \\ S(i_{qs1}) = i_{qs1}^{\ *} - i_{qs1}, \\ S(w_{r1}) = w_{r1}^{\ *} - w_{r1}. \end{cases} \tag{12}$$

For the second machine:

$$\begin{cases} S(i_{ds2}) = i_{ds2}^{\ *} - i_{ds2}, \\ S(i_{qs2}) = i_{qs2}^{\ *} - i_{qs2}, \\ S(w_{r2}) = w_{r2}^{\ *} - w_{r2}. \end{cases} \tag{13}$$

Deriving to the first order of (12) and (13), we obtain the following:

$$\begin{cases} \dot{S}(i_{dsi}) = \dot{i}_{dis}^{\ *} - \dot{i}_{dis}, \\ \dot{S}(i_{qsi}) = \dot{i}_{qis}^{\ *} - \dot{i}_{qis}, \\ \dot{S}(w_i) = \dot{w}_i^{\ *} - \dot{w}_i, \end{cases} \tag{14}$$

which

$$i = \begin{cases} 1 & \text{For the first machine,} \\ 2 & \text{For the second machine.} \end{cases}$$

A substitution of (3) and (5) into (14) leads to the following result:

$$\begin{cases} \dot{S}(i_{dsi}) = \dot{i}_{dis}^{\ *} - \dfrac{1}{L_{si} + L_{di}}\left(v_{dsi} - (R_{s1} + R_{s2})i_{dsi} + w_{ri}L_{qi}i_{qsi}\right), \\ \dot{S}(i_{qsi}) = \dot{i}_{qis}^{\ *} - \dfrac{1}{L_{si} + L_{qi}}\left(v_{qsi} - (R_{s1} + R_{s2})i_{qsi} - w_{ri}L_{di}i_{dsi} - \sqrt{\dfrac{5}{2}}w_{ri}\varphi_{fi}\right), \\ \dot{S}(w_{ri}) = \dot{w}_{ri}^{\ *} - \dfrac{p_i^{\ 2}}{J_{mi}}\left((L_{di} - L_{qi})i_{dsi} + \sqrt{\dfrac{5}{2}}\varphi_{fi}\right)i_{qsi} + \dfrac{p_i}{J_{mi}}T_{Li} + \dfrac{f_{mi}}{J_{mi}}w_{ri}. \end{cases} \tag{15}$$

The control strategy employs three variables, v_{dsi}, v_{qsi}, and i_{qsi}, as the control vector to drive the system toward the target condition where $S(x) = 0$. The corresponding equivalent control vector, expressed through v_{dieq}, v_{qieq}, and v_{qieq}, is obtained by $\dot{S}(x) = 0$, which yields the following relations for its elements:

$$\begin{cases} v_{dieq} = \left(L_{si} + L_{di}\right)\dot{i}_{dis}^{\ *} + (R_{s1} + R_{s2})i_{dsi} - w_{ri}L_{qi}i_{qsi}, \\ v_{qieq} = \left(L_{si} + L_{qi}\right)\dot{i}_{qis}^{\ *} + (R_{s1} + R_{s2})I_{qsi} + w_{ri}L_{di}i_{dsi} + \sqrt{\dfrac{5}{2}}w_{ri}\varphi_{fi}, \\ i_{qieq} = J_{mi}\dot{w}_{ri}^{\ *} + P_iT_{Li} + f_{mi}w_{ri} / (P_i((L_{di} - L_{qi})i_{dsi} + \sqrt{\dfrac{5}{2}}\varphi_{fi})). \end{cases} \tag{16}$$

The control vector is configured in this manner to guarantee effective performance and to achieve accurate dynamic response and switching behaviour on or in the vicinity of the surfaces:

$$\begin{cases} v_{dsi} = v_{dieq} + K \times sign\ (S(i_{dsi})), \\ v_{dsi} = v_{dieq} + K \times sign\ (S(i_{qsi})), \\ i_{qsi} = v_{qieq} + K \times sign\ (S(w_{ri})). \end{cases} \tag{17}$$

Although the discontinuous nature of the controller provides stability in the face of system uncertainties and external disturbances, it simultaneously generates high-frequency oscillations, a drawback referred to as chattering [22], [24].

IV. TOSMC APPROACH OF TWO SERIES-CONNECTED 5PH-PMSMS

A wide range of SMC methods have been developed; however, their real-world application is frequently limited by the issue of chattering. Studies have shown that higher-order SMC provides one of the most efficient solutions for minimising this unwanted phenomenon [22], [23].

The supertwisting SMC (STSMC) approach represents a second-order control method recognised for its strong robustness. Its main strengths lie in the simplicity of its design and its ability to operate effectively without requiring an exact mathematical model of the system. This characteristic enables it to handle parameter changes and external disturbances efficiently, while also delivering fast transient performance. For this reason, STSMC has become a widely adopted and extensively studied solution in the control of complex systems such as multiphase electric drives. A key feature of this method is that it is based solely on the sliding surface S, eliminating the need to evaluate the

sign of its derivative ($\dot{S}$) [29].

Although the STSMC technique has proven effective in theory, its application in electrical systems still faces considerable challenges. Implementing STSMC in drives, power converters, and multiphase machines often requires handling strong nonlinearities, fast dynamic behaviours, and wide operating conditions. These systems are also highly sensitive to measurement noise, discretisation effects, and implementation delays, which can limit the expected benefits of the controller. All of this is due to the chattering phenomenon [24], [29].

In this part, a novel control strategy is introduced to manage two series-connected five-phase PMSMs, where the use of third-order SMC (TOSMC) is used to improve the performance of the system compared to conventional MMS-based regulators. The proposed structure replaces the traditional controllers for both machines with dedicated TOSMC units, ensuring more accurate current and torque regulation. In addition, the outer control loop is redesigned by implementing a TOSMC-based speed controller, allowing coordinated regulation of the two motors under varying operating conditions.

The formulation of the TOSMC control signal is obtained by combining three separate terms, whose mathematical representation is provided in (18)

$$u(t) = u_1(t) + u_2(t) + u_3(t). \tag{18}$$

Accordingly, (19) is defined as follows:

$$\begin{cases} u_1(t) = \lambda_1 \sqrt{|S|}\, sign(S), \\ u_2(t) = \lambda_2 \int sign(S)dt, \\ u_3(t) = \lambda_3 sign(S), \end{cases} \tag{19}$$

where the switching function S defines the sliding surface. The parameters λ_1, λ_2, and λ_3 represent the adjusted positive gain values.

The schematic design adopted for constructing the TOSMC controller is shown in Fig. 3.

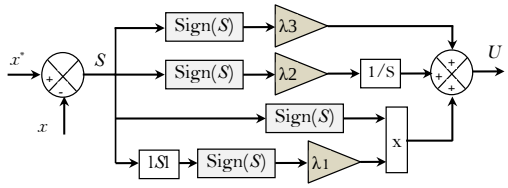

Fig. 3. The TOSMC controller.

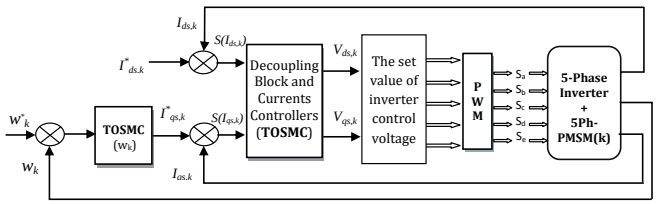

Fig. 4. Schematic of the proposed control strategy for two motors connected in series, with: k = 1 for the 5Ph-PMSM1, k = 2 for the 5Ph-PMSM2.

The error signals defined in (12) and (13) serve as inputs for the TOSMC controllers applied to both machines. In particular, the TOSMC based regulators for speed w_{ri} and currents i_{dsi} and i_{qsi} are employed to manage the reference torque T_{em}^*, as well as the stator voltage components v_{dsi} and v_{qsi}.

The control architecture of the system is illustrated in Fig. 4, which shows two series-connected 5Ph-PMSMs powered by a single five-phase inverter.

V. DISCUSSION AND RESULTS

The performance of the suggested control technique and the dynamic characteristics of a series-connected multimachine system (MMS) were investigated through numerical simulations using the MATLAB/SIMULINK platform. The simulation was configured with the parameters for both machines, as detailed in Table I [30]. This section assesses the effectiveness of the proposed TOSMC for the multimachine system (MMS-TOSMC) by comparing its outcomes against two benchmark controllers: a standard SMC (MMS-SMC) and a PI controller (MMS-PI). The evaluation is conducted through two primary examinations: reference tracking test under the effect of load torque T_r variation and to another verify the robustness of the controller against changes in machine parameters.

TABLE I. MACHINE PARAMETERS.

	5Ph-PMSM1	**5Ph-PMSM2**
Power	1.5 Kw	1.5 Kw
Stator resistance	R_{s1} = 0.67 Ω	R_{s2} = 0.67 Ω
Number of pairs poles	P_1 = 2	P_2 = 2
Inertia moment	J_{m1} = 0.004 Kg/m2	J_{m2} = 0.004 Kg/m^2
Stator inductances	$L_{d1} = L_{q1}$ = 0.0085 H	$L_{d2} = L_{q2}$ = 0.0085 H
Magnetic flux	ϕ_{f1} = 0.2 web	ϕ_{f2} = 0.2 web
Stator frequency	F_1 = 50 hz	F_2 = 50 hz

A. The First Test Case

This section aims to study how the regulators used in an MMS adapt to changes in operating conditions, such as external disturbances. To compare the responses of the controllers, we will use reference speed steps for each machine. The simulation established distinct speed profiles for two 5Ph-PMSMs. 5Ph-PMSM1 began at 150 rad/s, decelerated to 125 rad/s at 0.2 seconds, reversed to -125 rad/s at 0.8 seconds, and stopped at 1 second. Simultaneously, 5Ph-PMSM2 started at 125 rad/s, reduced to 100 rad/s at 0.2 s, was driven to -100 rad/s at 0.8 s, and also halted at t = 1 s. To evaluate performance under load, a torque of 5 Nm (designated T_{L1} and T_{L2}) is applied to both motors for a duration of between 0.4 and 0.6 seconds. Figures 5 and 6 illustrate the results of the current test.

Figures 5(a) and Figure 6(a) illustrate the rotation speeds, wr1 and wr2. We can conclude from two figures that all of the regulators follow the reference to rotation speed. The results demonstrate that the proposed MMS-TOSMC approach outperforms those of the standard MMS-PI and MMS-SMC in terms of tracking accuracy. The speed response time of the two machines using the proposed approach is the shortest among other MMS. For the first machine, the response time is estimated to be 0.0064 seconds using the proposed approach. This is in contrast to

the MMS-SMC and MMS-PI methods, which estimate response times to be 0.0116 and 0.0416 seconds, respectively. A similar performance advantage is observed for the 5Ph-PMSM2, where the proposed method results in a 0.0063-second response time, outperforming MMS-SMC (0.0093 seconds) and MMS-PI (0.0345 seconds).

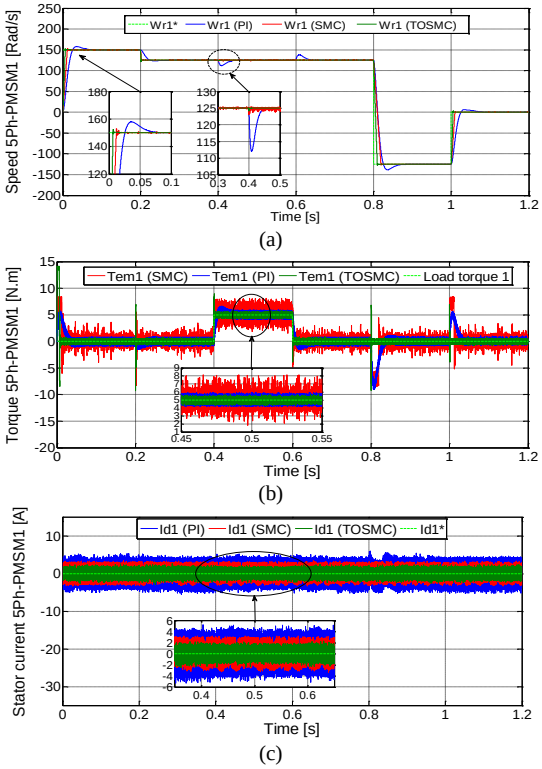

Fig. 5. Evaluation of reference tracking and load disturbance response of 5Ph-PMSM1 under different control approaches: (a) Rotation speed w_{r1}; (b) Electromagnetic torque T_{em1}; (c) Stator current I_{d1}.

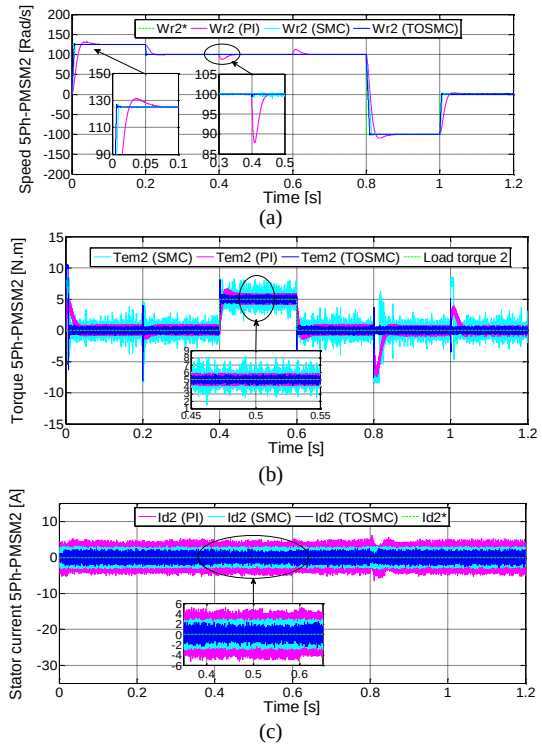

Fig. 6. Evaluation of reference tracking and load disturbance response of 5Ph-PMSM2 under different control approaches: (a) Rotation speed w_{r2}; (b) Electromagnetic torque T_{em2}; (c) Stator current I_{d2}.

The torque outputs (T_{em1} and T_{em2}) of the MMS are illustrated in Fig. 5(b) and Fig. 6(b). A comparison reveals that the proposed MMS-TOSMC approach is significantly more effective at suppressing torque fluctuations than both the conventional MMS-PI controller and the MMS-SMC method, which suffers from chattering. The proposed technique achieves a substantially lower torque ripple of just 1.5 Nm, compared to 1.65 Nm for the MMS-PI and 6.1 Nm for the MMS-SMC. This represents a reduction in torque ripple of approximately 9 % and 75.40 % for the 5Ph-PMSM1. For the second motor, the ripple was also considerably lower, showing reductions of 9.3 % and 76.03 % compared to the MMS-PI and MMS-SMC strategies, respectively. The results in Figs. 5(c) and 6(c) demonstrate that the proposed MMS-TOSMC method effectively drove the stator currents I_{d1} and I_{d2} close to zero, markedly outperforming other techniques.

B. The Second Test Case

To test the robustness of the proposed MMS-TOSMC strategy against parameter changes in the two motors, the evaluation was conducted using the reference tracking conditions for the first test. The resilience of the controllers was evaluated by introducing significant deviations in the main machine parameters: the stator resistances ($R_{s1,2}$) and the moments of inertia ($J_{1,2}$) were doubled, while the d-axis and q-axis inductances ($L_{d1,2}$ and $L_{q1,2}$) were decreased to 80 % of their original values. The results from this simulation are illustrated in Figs. 7 and 8.

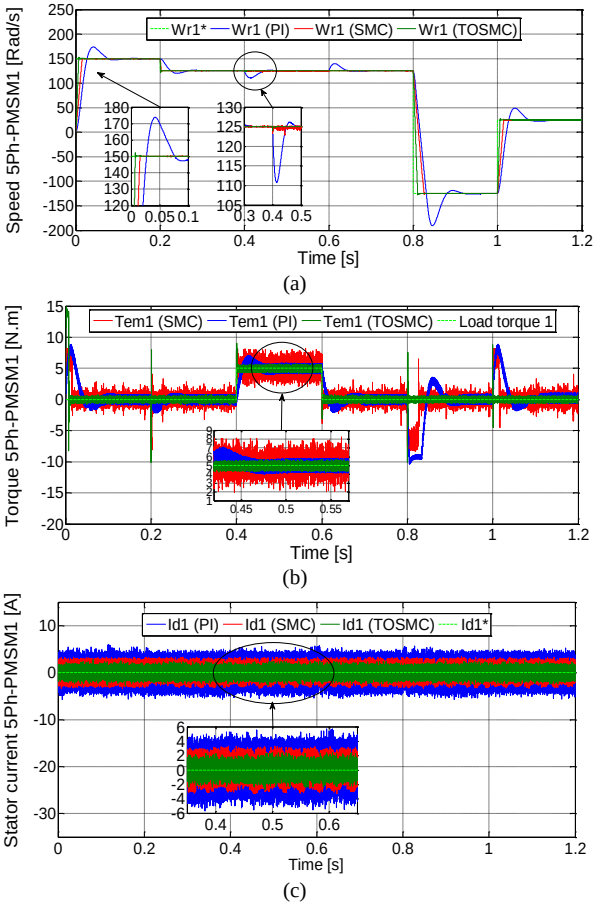

Fig. 7. Robustness test of the control methods for 5Ph-PMSM1: (a) Rotation speed w_{r1}; (b) Electromagnetic torque T_{em1}; (c) Stator current I_{d1}.

The performance comparison in Figs. 7(a) and 8(a) indicates that the proposed MMS-TOSMC controller is

more robust than the conventional MMS-PI controller when subjected to changes in machine parameters within a two-motor drive connected in series. The speed response of the MMS-PI controller was markedly less stable, exhibiting increased overshoot. This is quantified by the results: for 5Ph-PMSM1, the overshoot decreased from 174 rad/s using the traditional method to 152 rad/s with the new one. A similar improvement was seen in 5Ph-PMSM2, where the overshoot dropped from 145 rad/s to 126.5 rad/s.

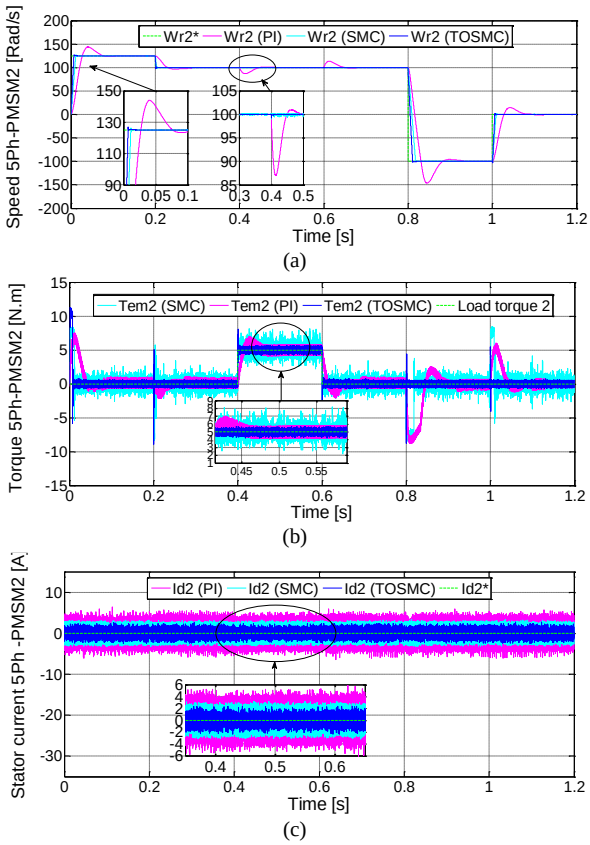

Fig. 8. Robustness test of control methods for 5Ph-PMSM2: (a) Rotation speed w_{r2}; (b) Electromagnetic torque T_{em2}; (c) Stator current I_{d2}.

The proposed MMS-TOSMC strategy delivers superior performance in minimising torque ripple, as evidenced by the significantly smoother electromagnetic torque outputs (T_{em1} and T_{em2}) shown in Fig. 7(b) and Fig. 8(b) when contrasted with conventional MMS-PI and MMS-SMC methods. As illustrated in Figs. 7(c) and 8(c), the proposed controller demonstrated superior performance in regulating current. It successfully maintained the stator currents I_{d1} and I_{d2} close to zero, a result that the alternative control strategies failed to achieve.

VI. CONCLUSIONS

In this study, a TOSMC-based nonlinear dynamic control strategy was developed to manage two series-connected five-phase PMSM powered by a single five-phase inverter. The proposed method was extensively validated through MATLAB/Simulink simulations and was benchmarked against the conventional MMS-PI and MMS-SMC approaches. Simulation results confirmed that the MMS-TOSMC design delivers notable improvements in the overall performance of the dual-motor system under various operating conditions. The TOSMC-based scheme introduced for MMS offers several key benefits:

– It ensures faster and more accurate tracking of reference speed and torque compared with the MMS-PI and MMS-SMC methods;

– It provides a smoother torque response with reduced ripples, which enhances efficiency and minimises acoustic noise;

– It exhibits stronger robustness against external disturbances, such as load variations and parameter mismatches, outperforming the conventional MMS-PI and MMS-SMC controllers.

Overall, the results highlight that the MMS-TOSMC approach represents an effective and reliable control framework for series-connected multimachine drive applications.

Future research will focus on experimental validation using real hardware, where the obtained results will be compared with those of different control techniques. In addition, future investigations will consider the integration of methods based on artificial intelligence for the control of multimachine systems connected in series.

CONFLICTS OF INTEREST

The authors declare that they have no conflicts of interest.

REFERENCES

[1] F. Tokgoz *et al.*, “Feasibility analysis of multiphase machines for electric vehicle applications”, *IEEE Transactions on Industry Applications*, vol. 61, no. 6, pp. 9216–9231, 2025. DOI: 10.1109/TIA.2025.3582566.

[2] Z. Liu *et al.*, “Experimental investigation of a real-time singularity-based fault diagnosis method for five-phase PMSG-based tidal current applications”, *ISA Transactions*, vol. 142, pp. 501–514, 2023. DOI: 10.1016/j.isatra.2023.07.038.

[3] A. Singh and A. Khosla, “A survey and analysis of multiphase electric propulsion motors and associated controllers for driving underwater platforms”, *Propulsion and Power Research*, vol. 14, no. 2, pp. 304–321, 2025. DOI: 10.1016/j.jppr.2025.06.001.

[4] M. Gholamian, O. Beik, and M. Arshad, “A Review of state-of-the-art multiphase and hybrid electric machines”, *Electronics*, vol. 13, no. 18, p. 3636, 2024. DOI: 10.3390/electronics13183636.

[5] M. Y. Metwly, A. S. Abdel-Khalik, M. S. Hamad, S. Ahmed, and N. A. Elmalhy, “Multiphase stator winding: New perspectives, advanced topologies, and futuristic applications”, *IEEE Access*, vol. 10, pp. 103241–103263, 2022. DOI: 10.1109/ACCESS.2022.3209372.

[6] D. Ghasemi, J. Siahbalaee, and M. Divandari, “Optimal control strategy of five-phase PMSMs in a wide speed range using third harmonics”, *International Transactions on Electrical Energy Systems*, vol. 2025, art. ID 4373929, pp. 1–17, 2025. DOI: 10.1155/etep/4373929.

[7] M. Sabna, V. P. Mini, S. Ushakumari, N. Mayadevi, and R. Harikumar, “A combined fault detection and diagnoses algorithm for open circuit faults and magnetic faults in a five-phase PMSM drive”, *e-Prime - Advances in Electrical Engineering, Electronics and Energy*, vol. 12, art. 100992, 2025. DOI: 10.1016/j.prime.2025.100992.

[8] T. Kamel, D. Abdelkader, B. Said, M. Al-Hitmi, and A. Iqbal, “Sliding mode control based DTC of sensorless parallel-connected two five-phase PMSM drive system”, *Journal of Electrical Engineering and Technology*, vol. 13, no. 3, pp. 1185–1201, 2018. DOI: 10.5370/JEET.2018.13.3.1185.

[9] G. Sun, G. Yang, J. Su, and G. Lu, “A flux–linkage torque ripple suppression method of dual–series FPMSMs decoupling control based on dual–frequency vector modulation”, *Energies*, vol. 15, no. 13, p. 4700, 2022. DOI: 10.3390/en15134700.

[10] T. J. dos Santos Moraes, M. Trabelsi, N. K. Nguyen, E. Semail, F. Meinguet, “Inverter fault diagnosis of an electrical series-connected two sinusoidal six-phase permanent magnet machines drive”, *IET Electric Power Applications*, vol. 14, no. 8, pp. 1412–1420, 2020. DOI: 10.1049/iet-epa.2019.0777.

[11] M. Nekkaz, A. Djahbar, and R. Taleb, “Modeling and control of two five-phase induction machines connected in series powered by matrix

converter", *International Journal of Power Electronics and Drive Systems*, vol. 12, no. 2, pp. 685–694, 2021. DOI: 10.11591/ijpeds.v12.i2.pp685-694.

[12] G. Boukhalfa, S. Belkacem, A. Chikhi, and M. Bouhentala, "Fuzzy-second order sliding mode control optimized by genetic algorithm applied in direct torque control of dual star induction motor", *Journal of Central South University*, vol. 29, no. 12, pp. 3974–3985, 2022. DOI: 10.1007/s11771-022-5028-3.

[13] E.-s. Terfia, S. Mendaci, S. E. Rezgui, H. Gasmi, and W. Kantas, "Optimal third-order sliding mode controller for dual star induction motor based on grey wolf optimization algorithm", *Heliyon*, vol. 10, no. 12, p. e32669, 2024. DOI: 10.1016/j.heliyon.2024.e32669.

[14] L. Zhang, M. Zhang, X. Zhu, C. Dong, and Z. Pei, "Adaptive harmonic decoupling sensorless control strategy of a new five-phase flux-intensifying permanent magnet motor under healthy and faulty conditions", *IEEE Journal of Emerging and Selected Topics in Power Electronics*, vol. 12, no. 1, pp. 1078–1087, 2024. DOI: 10.1109/JESTPE.2023.3342429.

[15] Q. Chen, J. Chen, H. Shi, L. Fu, and G. Liu, "Flux weakening control of dual five-phase hybrid excitation permanent magnet synchronous motor", *IEEE Transactions on Transportation Electrification*, vol. 11, no. 4, pp. 10415–10426, 2025. DOI: 10.1109/TTE.2025.3565923.

[16] M. A. Mossa, H. Echeikh, N. El Ouanjli, and H. H. Alhelou, "Enhanced second-order sliding mode control technique for a five-phase induction motor", *International Transactions on Electrical Energy Systems*, vol. 2022, art. ID 8215525, pp. 1–19, 2022. DOI: 10.1155/2022/8215525.

[17] Y. Wu, Z. Zhang, Q. Yang, W. Tian, P. Karamanakos, M. L. Heldwein, and R. Kennel, "A direct model predictive control strategy with an implicit modulator for six-phase PMSMs", *IEEE Journal of Emerging and Selected Topics in Power Electronics*, vol. 11, no. 2, pp. 1291–1304, 2023. DOI: 10.1109/JESTPE.2022.3170847.

[18] F. Mehedi, I. Bouyakoub, A. Yousfi, and Z. Reguieg, "Enhanced control technique based on fuzzy logic algorithms for a five-phase induction motor fed by a multilevel inverter", *IJE TRANSACTIONS B: Applications*, vol. 38, no. 2, pp. 351–361, 2025. DOI: 10.5829/ije.2025.38.02b.09.

[19] P. Rajanikanth and V. K. Thippiripati, "An improved model predictive current control of five-phase PMSM drive for torque and flux ripple alleviation", *IEEE Journal of Emerging and Selected Topics in Industrial Electronics*, vol. 5, no. 3, pp. 1273–1282, 2024. DOI: 10.1109/JESTIE.2024.3389293.

[20] H. H. Boughezala, K. Laroussi, S. Khadar, A. S. Al-Sumaiti, and M. A. Mossa, "Optimized sensorless control of five-phase permanent magnet synchronous motor using a genetic algorithm-Real time implementation", *IEEE Access*, vol. 12, pp. 98367–98378, 2024. DOI: 10.1109/ACCESS.2024.3429181.

[21] L. Zhang, C. Dong, X. Zhu, X. Chen, and Z. Pei, "A fault-tolerant MTPA control strategy of five-phase flux-intensifying fault-tolerant permanent-magnet motor with sliding-mode disturbance observer under open-circuit and short-circuit faults", *IEEE Transactions on Industrial Electronics*, vol. 71, no. 11, pp. 13650–13658, 2024. DOI: 10.1109/TIE.2024.3363722.

[22] X. Liu, Y. Deng, J. Liu, H. Cao, C. Xu, and Y. Liu, "Fixed-time integral terminal sliding mode control with an adaptive RBF neural network for PMSM speed regulation", *Control Engineering Practice*, vol. 156, art. 106236, 2025. DOI: 10.1016/j.conengprac.2024.106236.

[23] N. M. Alyazidi, A. F. Bawazir, and A. S. Al-Dogail, "Robust integral sliding mode control for pressure management in multi-phase flow systems", *Results in Engineering*, vol. 25, art. 104024, 2025. DOI: 10.1016/j.rineng.2025.104024.

[24] B. Sabouni, K. Makhloufi, M. Zerikat, B. Bouchiba, and I. K. Bousserhane, "Experimental verification of a fuzzy adaptive sliding mode control design for IM speed control", *Periodica Polytechnica Electrical Engineering and Computer Science*, vol. 69, no. 3, pp. 236–250, 2025. DOI: 10.3311/PPee.39509.

[25] D. Zellouma, Y. Bekakra, and H. Benbouhenni, "Robust synergetic-sliding mode-based-backstepping control of induction motor with MRAS technique", *Energy Reports*, vol. 10, pp. 3665–3680, 2023. DOI: 10.1016/j.egyr.2023.10.035.

[26] J. Duan, S. Wang, and L. Sun, "Backstepping sliding mode control of a permanent magnet synchronous motor based on a nonlinear disturbance observer", *Applied Sciences*, vol. 12, no. 21, p. 11225, 2022. DOI: 10.3390/app122111225.

[27] M. A. Khoshhava, H. A. Zarchi, and G. A. Markadeh, "Sensor-less speed and flux control of dual stator winding induction motors based on super twisting sliding mode control", *IEEE Transactions on Energy Conversion*, vol. 36, no. 4, pp. 3231–3240, 2021. DOI: 10.1109/TEC.2021.3077829.

[28] H. Moussa, S. Krim, H. Kesraoui, M. Mansouri, and M. F. Mimouni, "Loss model control for efficiency optimization and advanced sliding mode controllers with chattering attenuation for five-phase induction motor drive", *Energies*, vol. 17, no. 16, p. 4192, 2024. DOI: 10.3390/en17164192.

[29] A. Ullah, S. Ullah, Z. Zhang, and P. Jianfei, "Smooth super-twisting sliding mode control design with high order super-twisting observer for speed tracking control of permanent magnet synchronous motor drive system", *ISA Transactions*, vol. 162, pp. 227–242, 2025. DOI: 10.1016/j.isatra.2025.04.007.

[30] M. A. Mossa, H. Echeikh, and A. Ma'arif, "Dynamic performance analysis of a five-phase PMSM drive using model reference adaptive system and enhanced sliding mode observer", *Journal of Robotics and Control*, vol. 3, no. 3, pp. 289–308, 2022. DOI: 10.18196/jrc.v3i3.14632.